Spin excitations in $K_2Fe_{4+x}Se_5$: linear response approach

Liqin Ke,[1] Mark van Schilfgaarde,[2] and Vladimir Antropov[1]
[1]*Ames Laboratory USDOE, Ames, IA 50011*
[2]*Department of Physics, King's College London, Strand, London WC2R 2LS*
(Dated: March 5, 2013)

Abstract

Using *ab initio* linear response techniques we calculate spin wave spectra in $K_2Fe_{4+x}Se_5$, and find it to be in excellent agreement with a recent experiment. The spectrum can be alternatively described rather well by localized spin Hamiltonian restricted to first and second nearest neighbor couplings. We confirm that exchange coupling between nearest neighbor Fe magnetic moments is strongly anisotropic, and show directly that in the ideal system this anisotropy has itinerant nature which can be imitated by introducing higher order terms in effective localized spin Hamiltonian (biquadratic coupling). In the real system, structural relaxation provides an additional source of the exchange anisotropy of approximately the same magnitude. The dependence of spin wave spectra on filling of Fe vacancy sites is also discussed.

Because there seems to be a close, if poorly understood, connection between magnetic excitations and superconductivity in the recently discovered families of Fe-based superconductors, a great deal of attention has been paid to the elementary magnetic excitations in these systems[1, 2]. While the number of materials with superconducting properties is rapidly growing, they all share in common a phase diagram with an antiferromagnetic region immediately adjacent to the superconducting phase. AFM order in most parent compounds are characterized by rather steep spin waves (antiferromagnons) and relatively low Néel temperature ($\sim$140 K) [1, 2]. On the other hand, iron selenides $K_2Fe_{4+x}Se_5$ discovered very recently, which we will call here a "245" system, is a particularly interesting case, because while its superconducting state appears to be similar in many respects to some of the other families, has a much higher Néel temperature ($T_N \sim 560K$) and very large magnetic moment ($\sim 3\mu_B$) [3–5]. The first neutron experiments, performed only recently [6], show collective spin excitations somewhat similar to excitations in the Fe-pnictides such as $CaFe_2As_2$. A highly debated topic of discussion is the anisotropy of the exchange coupling. In Ref. [6] the authors fit a set of anisotropic Heisenberg model parameters to their data, and argued that at least three effective nearest neighbor (NN) exchange parameters are needed to fit observed spectra in a satisfactory manner. In another recent work [7] this exchange anisotropy has been fully attributed to biquadratic exchange, supporting the model introduced in Ref. [6]. However, neutron linear response experiments do not contain sufficient information to establish whether or not higher order terms of localized spin Hamiltonian or other interactions are responsible for this anisotropy. Information from the linear regime cannot unambiguously distinguish the dependence of linear response behavior on environment and terms originating from higher order. The unique answer can be obtained using non-collinear band structure calculations together with a linear response theory [8].

Here we analyze spin excitations in the 245 system using non-collinear density functional theory in tandem with a linear response approach to determine the spin wave (SW) spectra of both the parent compound, $K_2Fe_4Se_5$, and its modification by addition of Fe on the 'vacancy' sites as described below. We accurately reproduce observed features in SW spectra of the parent compound from this first principles approach, without recourse to empirical or adjustable parameters. Thus we argue that the Heisenberg model extracted from this theory provides a good description of the static transverse susceptibility, and the exchange parameters J_{ij} derived *ab initio* from it, which have a physical meaning as the second variation in total energy with respect to spin rotations, are accurately given by the theory. We can also unambiguously address what happens when exchange parameters, which can be computed to whatever range is desired, are truncated to a short range, e.g. just first and second neighbors (J_1–J_2 model).

For computational convenience we adopt a multiple-scattering approach in the long wave approximation [9], which is reasonable provided the local Fe moment is sufficiently large. This is the case in $K_2Fe_{4+x}Se_5$, where the Fe local moment is both measured to be $\sim 3\mu_B$, and predicted to be so in density-functional theory.

The parent compound $K_2Fe_4Se_5$ has a vacancy on the Fe sublattice for each formula unit, which if filled would have a composition $K_2Fe_5Se_5$ and be structurally similar to the other Fe superconductors. The ordered magnetic phase of $K_2Fe_4Se_5$ is unusual: blocks of four Fe atoms are coupled ferromagnetically in a square; the squares are arranged antiferromagnetically in a Néel like configuration, which we denote the "block Néel" magnetic structure. In what manner the vacancy Fe sites are filled in superconducting material is a crucial issue, because the parent compound is predicted in density-functional theory to be an insulator with a bandgap of $\sim$0.4 eV [10].

We first consider magnetic excitations of the parent compound, with reciprocal lattice vectors G_1=(0.4,−0.2,0), G_2=(0.2,0.4,0), and G_3=(0,0,a/c), in units of $2\pi/a$. This cell contains four formula units of $K_2Fe_4Se_5$ with two units per plane. We used experimental lattice constants from Ref. [11] with a=3.914Å, and c/a=3.587. Because the LDA is known to underestimate Fe-chalcogen and Fe-pnictogen bond lengths in

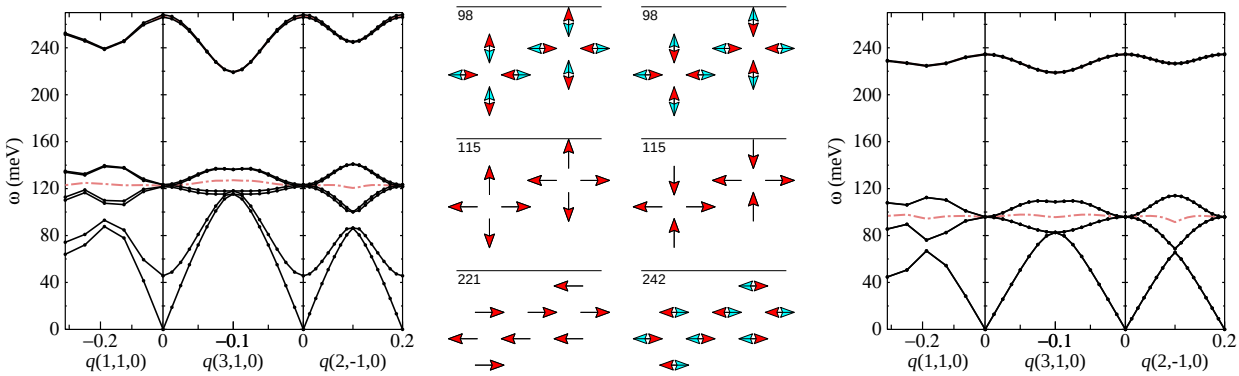

FIG. 1: Spin-wave spectra in $K_2Fe_4Se_5$ calculated from the static susceptibility in the LDA. Panel (a) shows $\omega(q)$, with the right frame for q along the $\Gamma-G_1$ line. It corresponds to the experimental spectra shown in Ref. [6] (bottom panels of Fig. 3), whereas the left frame corresponds to the top panel of that Figure. The middle frame shows spectra along the $\Gamma-(G_1+G_2)$ line. Panel (b) shows eigenvectors of the six optical modes at Γ, and their corresponding frequencies (meV). The perspective is from the z axis, so each point contains two Fe atoms. Arrows corresponding to spin rotations of each of the 16 Fe atoms. In some panels only 8 arrows are visible; this occurs when the rotations in the upper and lower planes are in phase. In other panels all 16 arrows are visible; for these modes the lower and upper planes are 180° out of phase. The right frame shows how the SW get modified when the exchange interactions are restricted to J_1 and J_2 only.

TABLE I: Bond lengths (Å) of $K_2Fe_4Se_5$ in the block Né structures calculated from PBE and LDA functionals, bandgap (eV) and magnetic moment M (μ_B). "LDA@PBE" refers to calculations using the Barth-Hedin (local) functional, but calculated at the PBE minimum-energy geometry. The shorter (longer) of the Fe-Fe bond length is the intrablock (interblock) distance. Mean PBE Fe-Fe and Fe-Se bond lengths are close to the experimental values. "25% Fe" refers to an LDA@PBE calculation with 25% doping of the Fe vacancy sites, as discussed in the text.

	d(Fe-Fe)	d(Fe-Se)	E_g	M
Expt	2.768	2.441		3.3
PBE	2.657–2.901	2.406–2.509	0.59	3.02
LDA	2.649–2.872	2.354–2.454	0.26	2.75
LDA@PBE			0.44	2.90
25% Fe	2.604–2.814	2.399–2.518	0.01	2.3–2.9

these families of superconductors, we use the PBE functional to relax the crystal structure in the block Néel magnetic state. The resulting relaxed structure, is seen in Table I to agree well with experimental data. On the other hand, the PBE functional tends to overestimate the magnetic moments and magnetic stabilization energy. Thus to calculate magnetic excitations, we use the LDA, but adopt the crystal structure predicted by the PBE functional.

The full susceptibility $\chi^{-1}(\mathbf{q},\omega)$ is prohibitively expensive to calculate for such a large system. Thus we adopt an approach which relies on the atomic sphere approximation (ASA) following Ref. [12]. To check ASA approximation to DFT, we carefully checked the energy bands, density of states, and magnetic moment in ASA against LDA results and found satisfactory agreement for all cases described here; for example the ASA bandgap and magnetic moment of the parent compound were found to be 0.40 eV and 2.85μ_B, close to the LDA@PBE result of Table I.

Pair exchange parameters J_{ij} were obtained from a Fourier transform of $J(\mathbf{q})$; the latter was calculated on fine a q-mesh of 16×16×4 divisions in order to reliably extract J_{ij} to very distant neighbors. Resulting spin wave spectra for the parent compound $K_2Fe_4Se_5$ are shown in Fig. 1. Focusing first on the Γ point, six optical modes are seen: two degenerate pairs clustered around 100 meV, and two others near 230 meV. (We defer discussion of the mode near 40 meV for the moment.) The middle panel of Fig. 1 depicts their eigenvectors. The lowest pair and second pair are essentially the same in a given plane, but top and bottom planes rotate against each other for the low-energy pair, and in phase for the high energy pair. The first high-energy mode consists uniform rotations spins against parallel sheets on the xz axis; the second is similar but upper and lower planes are out of phase.

Left and right frames can be compared directly with neutron data, top and bottom panels of Fig. 3 of Ref. [6]. All modes match experimental data very well, when broadening in the experimental spectrum is taken into account. The acoustic mode, with linear dispersion for small q of Fig. 1 has a maximum of 86 meV at q=(1/2)G_1, slightly larger than the measured value in Ref. [6]. The four low-energy optical modes are all "breathing" modes: spins rotate radially away from the center of their square. These four separate modes cannot be resolved in experiment; instead the measured data reflects a superposition of these modes. It is nearly dispersionless along the $\Gamma-G_1$ line, with $\omega\approx$110 meV. For comparison to experiment four optical modes were averaged and shown as a dashed line in Fig. 1, and the result is seen to be the same as the neutron data, though at slightly higher energy. Finally the two high-energy optical modes show a

TABLE II: Exchange energies J_k, in meV, for the Heisenberg hamiltonian $H=\sum J_{ij}\,\mathbf{S}_i\cdot\mathbf{S}_j$, of the parent compound $K_2Fe_4Se_5$. Here k denotes the neighbor index. J_k and J'_k refer to couplings between pairs of like spin and opposite spin, respectively. Also shown is the Néel temperature, estimated from the RPA [13].

	Relaxed geometry		Ideal geometry	
k	J_k	J'_k	J_k	J'_k
1	-9.7	27.3	-5.7	25.7
2	10.2	8.5	17.0	6.7
3	0.3	-0.3	0.1	-0.1
4	-1.9	0.1±1.0	-2.2	0.5±0.5
5	0.1	0.5	-0.3	0.5
6	-0.1	0.1±0.1		0.1±0.1
7	-0.1	1.3		
T_N	494 K		(not stable)	

weak q dependence, with $\omega\approx$240 meV. Essentially identical behavior is observed in the neutron data along the (110) line, though ω is slightly smaller. The Néel temperature, T_N, estimated within the RPA, is about 12% smaller than the observed value. This is in fact very good agreement with experiment, since the RPA is known to underestimate critical temperatures for a given Hamiltonian, by roughly 10%.

Finally, consider the mode appearing near 40 meV. If the two Fe planes were identical and uncoupled this mode would exactly coincide with the acoustic mode. Thus it is essentially the acoustic mode with q_z=$1/2\cdot 2\pi/c$, zone-folded to the Γ point, because the actual crystal contains two planes of Fe. The splitting of this and the true acoustic mode are a result of coupling between the two planes through exchange parameters along J^z coupling different planes. This shows that J^z is small, but not so small that planes are decoupled.

A great deal of speculation has arisen in the community about the size and range of parameters J. Much effort has been expended extracting effective exchange parameters J_{ij} by fitting a Heisenberg model with a few (2 or 3) neighbors to the observed data, as was done in Refs. [6] and [7]. Since, as we have shown, SW can well described by the Heisenberg model derived *ab initio*, these results enable us to unambiguously address questions about the range and environment dependence of J_{ij}. In particular, it is debated whether a J_1–J_2 model is sufficient or more distant neighbors are required. Table II shows J_{ij} for the first few neighbors, distinguishing intra-block and interblock couplings. As widely thought, the first two neighbors give by far the largest contribution to J. To quantify this effect, we recalculated the SW spectrum with J restricted to only nearest and second neighbor. This leaves four independent parameters since interblock J and intrablock J' are distinct (Table II). The resulting SW spectra, shown in the right panel of Fig. 1, look qualitatively similar to the full calculation, except that some modes become degenerate, and low-energy modes soften by about 25%. The predicted T_N drops by a comparable amount, from 494K to 399K. Perhaps most importantly, the "zone-folded" acoustic mode noted above becomes degenerate with the true acoustic mode, because all interplane interactions are now excluded by construction.

Remarkably, corrections to the J_1–J_2 approximation receive almost *no* contribution from J_3; rather, they originate from J_4–J_7 (especially J'_7). The magnetic structure is stabilized by strong AFM first and second neighbor interblock coupling, and weakly so by nearest intrablock exchange. Frustration is present, since the AFM second neighbor intrablock coupling acts strongly to destabilize the magnetic order, but it is overcome because there are half as many such pairs as their interblock counterparts. The Table also shows what J_{ij} would obtain if the structure were constrained to an ideal geometry. Relaxation causes a small deformation of the Fe atoms in squares; there is also some dispersion in the Fe-Se bond length around the average value (Table I). This structural relaxation is critically important for magnetic stability. As Table II shows, the stability of the (intrablock) square is strongly enhanced by relaxation: the NN coupling is increased and frustration in the 2nd NN is strongly reduced. Without relaxation some of SW frequencies become complex, indicating that the collinear state is not stable.

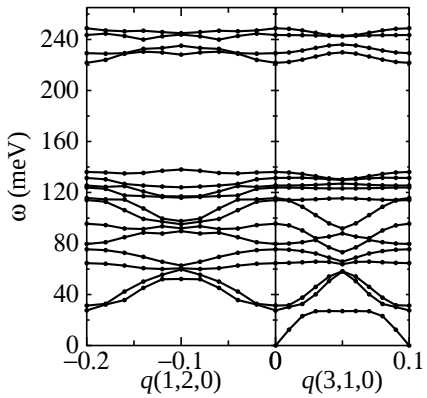

FIG. 2: Spin-wave spectra for $K_2Fe_{4.25}Se_5$ as described in the text. Actual cell is $K_{16}Fe_{34}Se_{40}$.

As the filling of Fe vacancy sites very likely play an essential role in mediating superconductivity, how elementary excitations are modified when these sites are partially occupied is a crucial question. We consider first 25% occupation of Fe vacancies. To retain an overall zero-spin configuration it is necessary to double the size of the four formula unit cell: we construct a supercell with G_1=(0.3,0.1,0) and G_2=(−0.1,0.3,0), and populate two of the eight vacancy sites with a pair of $Fe^{\uparrow}$ and $Fe^{\downarrow}$ atoms in such a way as to preserve a two-fold rotational symmetry. The lattice was relaxed using the PBE functional, with the resulting equilibrium bond lengths shown in Table I. SW's are shown in Fig. 2. The acoustic mode (now zone folded) is largely unchanged and uncoupled from the other modes: there is a linear dispersion at small q and a maximum near 80 meV for, e.g. $\mathbf{q}$=(0.3,0.1,0)

and $\mathbf{q}$=(0.1,−0.2,0). The (zone-folded) low-energy optical modes now show some new features. In addition to the modes in the 80-120 meV range, new and largely dispersionless modes appear around 60 meV. The eigenfunctions of these modes are very complex, with strong admixtures of both vacancy sites and host sites. The high-frequency modes are almost unchanged as "vacancy" Fe atoms participate very little in them.

At 25% filling the magnetic structure is stable; indeed T_N for $K_2Fe_4Se_5$, predicted to be 494 K in the Tyablikov approximation, is only slightly reduced, to 485K for $K_2Fe_{4.25}Se_5$. We also studied a case with 50% filling. A collinear magnetic state was stabilized; however the linear response calculation of the SW spectra revealed imaginary frequencies, indicating that the collinear state is not stable.

The exchange anisotropy, $J_k - J'_k$, is unusually large in this material. It is natural to associate $J_k - J'_k$ with biquadratic coupling, as was done in Refs.[14]. However, lattice relaxations are very important in this case; compare the ideal to relaxed J in Table II. Our calculations predict that the intrablock NN Fe-Fe bond length is calculated to be smaller than the intrablock one by ∼8% (Table I); and perhaps more important, there is a significant dispersion in the Fe-Se bond lengths. The strictly electronic part of biquadratic contribution is still present and our calculations for the ideal 245 (no relaxation) show that biquadratic coupling is about 30% of J_1. This result was obtained by set of calculations of non-collinear configurations that enable us to go beyond linear response. We fit the total energy of the different non-collinear states to effective spin Hamiltonian with higher order terms and found a large $\cos^2\theta$ contribution from first NN, while contribution from higher harmonics appeared to be smaller. Also biquadratic coupling from the second NN is smaller. Thus the environment dependence of J originates from two sources: purely electronic terms for a fixed lattice, and an "exchange-striction" contribution, originating from spin-configuration-dependent lattice relaxation.

These non-collinear calculations point to the microscopic origin of the biquadratic interaction. It appears that major contribution to this 'biquadratic' energy is produced by the change of the amplitude of magnetic moments. M was found to vary by $\sim 0.3\mu_B$, even though its magnitude is large and thought to be well described by a rigid local-moment picture. The presence of unusually large interaction between longitudinal and transverse degrees of freedom reflects the relatively large itinerant component of magnetic interactions in this system. It is notable that the interaction between these kinds of fluctuations lies outside a linear response description. The LDA is a mean-field theory and does not incorporate fluctuations directly. It can nevertheless capture some aspect of fluctuations through the imposition of constraints (spin orientations).

In conclusion, we demonstrated that *ab-initio* linear response method nearly perfectly describes the observed spin wave spectra in the complicated 245 system. The experimental spectrum alternatively can be described reasonably well by localized spin Hamiltonian with two nearest neighbor couplings. We confirm the anisotropy of the exchange coupling between NN Fe magnetic moments and established that this anisotropy is associated with significant biquadratic coupling which appears in part because of longitudinal fluctuations. Structural relaxation provides an additional source of the exchange anisotropy of approximately the same magnitude.

Work at the Ames Laboratory was supported by DOE Basic Energy Sciences, Contract No. DE-AC02-07CH11358.

[1] D. C. Johnston, Advances in Physics **59**, 803 (2010).
[2] J. W. Lynn and P. Dai, Physica C: Superconductivity **469**, 469 (2009).
[3] W. Bao, G. N. Li, Q. Huang, G. F. Chen, J. B. He, M. A. Green, Y. Qiu, D. M. Wang, and J. L. Luo, ArXiv e-prints (2011), 1102.3674.
[4] P. Zavalij, W. Bao, X. F. Wang, J. J. Ying, X. H. Chen, D. M. Wang, J. B. He, X. Q. Wang, G. F. Chen, P.-Y. Hsieh, et al., Phys. Rev. B **83**, 132509 (2011).
[5] B. Wei, H. Qing-Zhen, C. Gen-Fu, M. A. Green, W. Du-Ming, H. Jun-Bao, and Q. Yi-Ming, Chin. Phys. Lett. **28**, 086104 (2011).
[6] M. Wang, C. Fang, D.-X. Yao, G. Tan, L. W. Harriger, Y. Song, T. Netherton, C. Zhang, M. Wang, M. B. Stone, et al., Nature Commun. **2**, 580 (2011).
[7] J. Hu, B. Xu, W. Liu, N.-N. Hao, and Y. Wang, Phys. Rev. B **85**, 144403 (2012).
[8] T. Kotani and M. van Schilfgaarde, J. Phys.: Conden. Matter **20**, 295214 (2008).
[9] V. Antropov, J. Magn. Magn. Mater. **262**, L192 (2003).
[10] C. Cao and J. Dai, Phys. Rev. Lett. **107**, 056401 (2011).
[11] Z. Wang, Y. J. Song, H. L. Shi, Z. W. Wang, Z. Chen, H. F. Tian, G. F. Chen, J. G. Guo, H. X. Yang, and J. Q. Li, Phys. Rev. B **83**, 140505 (2011).
[12] M. van Schilfgaarde and V. P. Antropov, J. Appl. Phys. **85**, 4827 (1999); V. P. Antropov, M. van Schilfgaarde, S. Brink, and J. L. Xu, J. Appl. Phys. **99**, 08F507 (2006).
[13] V. Antropov, B. Harmon, and A. Smirnov, J. Magn. Magn. Mater. **200**, 148 (1999).
[14] J. Pulikkotil, L. Ke, M. van Schilfgaarde, T. Kotani, and V. Antropov, Superconductor Science and Technology **23**, 054012 (2010); A. L. Wysocki, K. D. Belashchenko, and V. P. Antropov, Nature Phys. **7**, 485 (2011).